



Dimensional Accuracy and Repeatability of Mould Inserts Manufactured by Mask Projection Vat-Photopolymerization

Bertelsen, J. G. ; Thorn, S. ; Mendez Ribo, Macarena; Li, D. ; Regi, Francesco; Davoudinejad, Ali; Zhang, Yang; Tosello, Guido

Publication date:
2018

Document Version
Publisher's PDF, also known as Version of record

[Link back to DTU Orbit](#)

Citation (APA):
Bertelsen, J. G., Thorn, S., M. Ribo, M., Li, D., Regi, F., Davoudinejad, A., ... Tosello, G. (2018). Dimensional Accuracy and Repeatability of Mould Inserts Manufactured by Mask Projection Vat-Photopolymerization. Poster session presented at Euspen Special Interest Group Meeting 2018: Structured & Freeform Surfaces, Cachan, France.

General rights

Copyright and moral rights for the publications made accessible in the public portal are retained by the authors and/or other copyright owners and it is a condition of accessing publications that users recognise and abide by the legal requirements associated with these rights.

- Users may download and print one copy of any publication from the public portal for the purpose of private study or research.
- You may not further distribute the material or use it for any profit-making activity or commercial gain
- You may freely distribute the URL identifying the publication in the public portal

If you believe that this document breaches copyright please contact us providing details, and we will remove access to the work immediately and investigate your claim.

Dimensional Accuracy and Repeatability of Mould Inserts Manufactured by Mask Projection Vat-Photopolymerization

J.G. Bertelsen^{†1}, S. Thorn^{†1}, M.M. Ribo¹, D. Li¹, F. Regi¹, A. Davoudinejad¹, Y. Zhang¹, G. Tosello¹

[†]These authors contributed equally to this work. ¹Technical University of Denmark (DTU)

Motivation

Introduction

Mask projection vat-photopolymerisation (MPVP) technology provides a method for additive manufacturing (AM) of high resolution surface features. In the present project, the technology is used to generate injection moulding inserts containing a double-curved freeform surface with bi-directional reflectance patterns (Fig. 1 & 2). Orienting the anisotropic patterns by 0° and 90° relative to the viewing direction generates surface contrast with “dark” and “bright” areas (Fig. 5). This allows for incorporation of information barcodes in the polymer insert which subsequently replicates into every injection moulded part, e.g. enhanced product traceability, B2B information or end-user interaction.

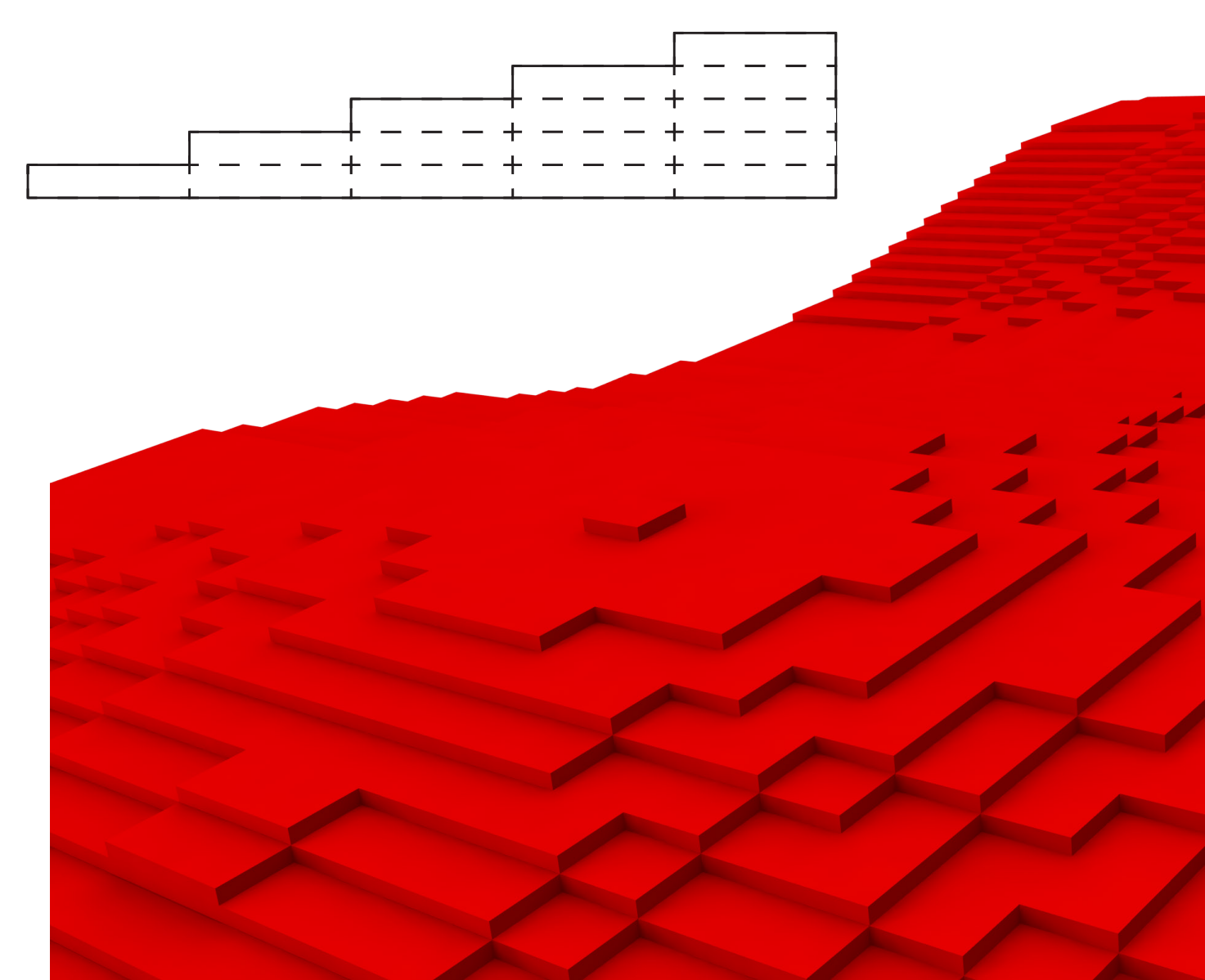


Fig. 1. Initial CAD model of double curved freeform surface without reflectance elements. Render from SolidWorks 2018 Photoview 360.

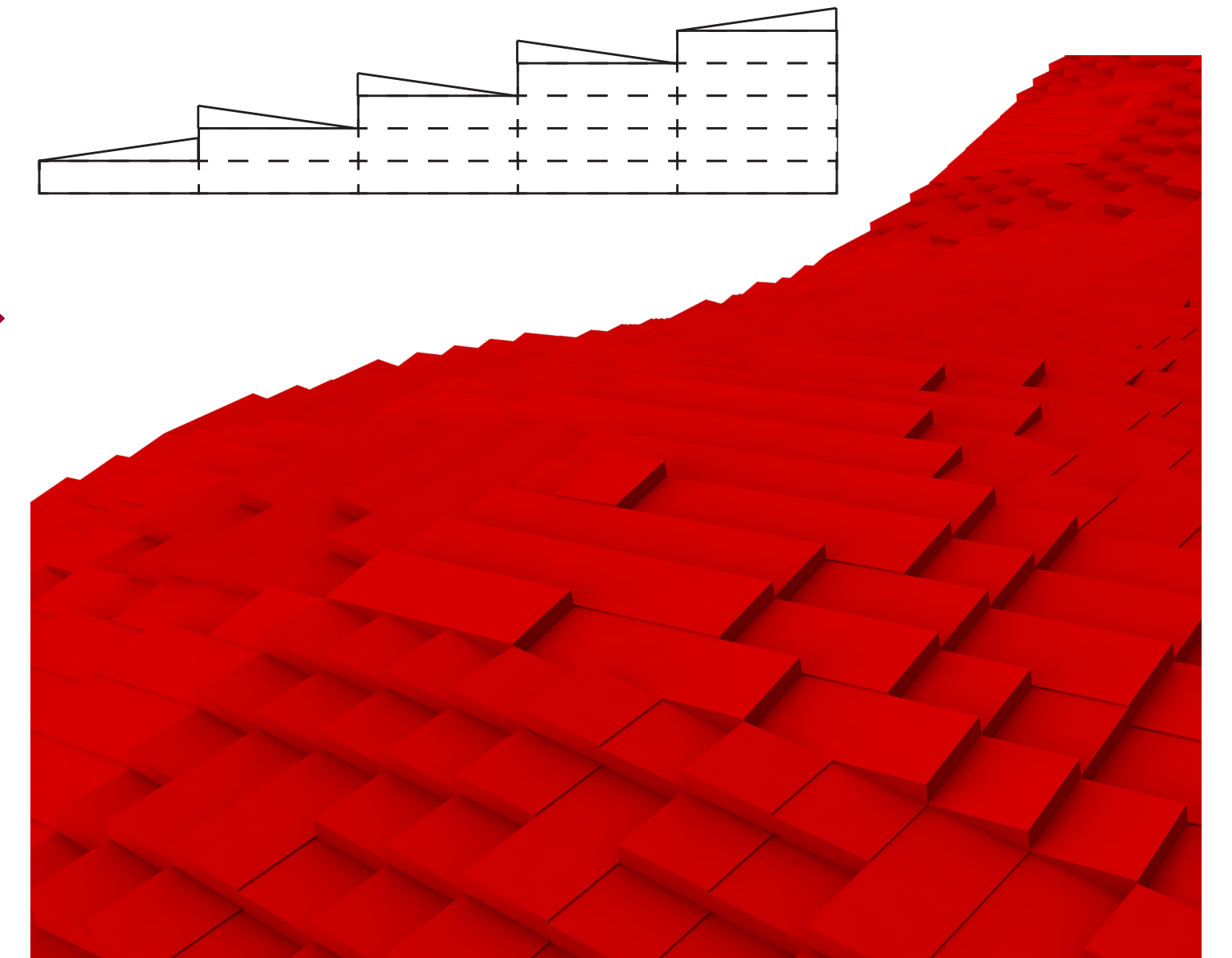


Fig. 2. Final CAD model including reflectance elements. The viewing angle is identical to Fig. 1. Render from SolidWorks 2018 Photoview 360.

Results & Findings

Parameter optimisation

A study of optimal parameters has been conducted with a “working curve experiment”. Cure depth C_d is plotted as a function of radiant exposure E with a logarithmic behavior (Fig. 3 & 4) - in full accordance with the Beer-Lambert Law. The slope is the penetration depth D_p (the depth at which the irradiance is reduced to $1/e$ (~37 %) of the surface irradiance) and the intersection with the x-axis is the critical exposure E_c that causes gelation/cross-linking. The results from the working curves were used in a subsequent full-factorial, two-level DoE to reveal specific parameters to achieve best replication of surface features.

Resulting surfaces

CAD part and printed features were in close concordance at $E = 11.83 \text{ mJ/cm}^2$, however areas from midline to peak were not printed correctly due to overexposure. Using $E = 1.94 \text{ mJ/cm}^2$ generates a uniformly covered reflectance surface with fewer defects (Fig. 6). Metrological assessment of parts created with $1 \mu\text{m}$ and $0.625 \mu\text{m}$ layer thickness yield low surface roughness with R_a values ~10-50 nm (Fig. 7 & Tab. 1). The process generally yields more defects at layer thickness below $4 \mu\text{m}$. This instability could be due to oxygen inhibition, insufficient stirring due to capillary forces and varying detachment area.

Working curve FunToDo Industrial Blend Red (logarithmic)

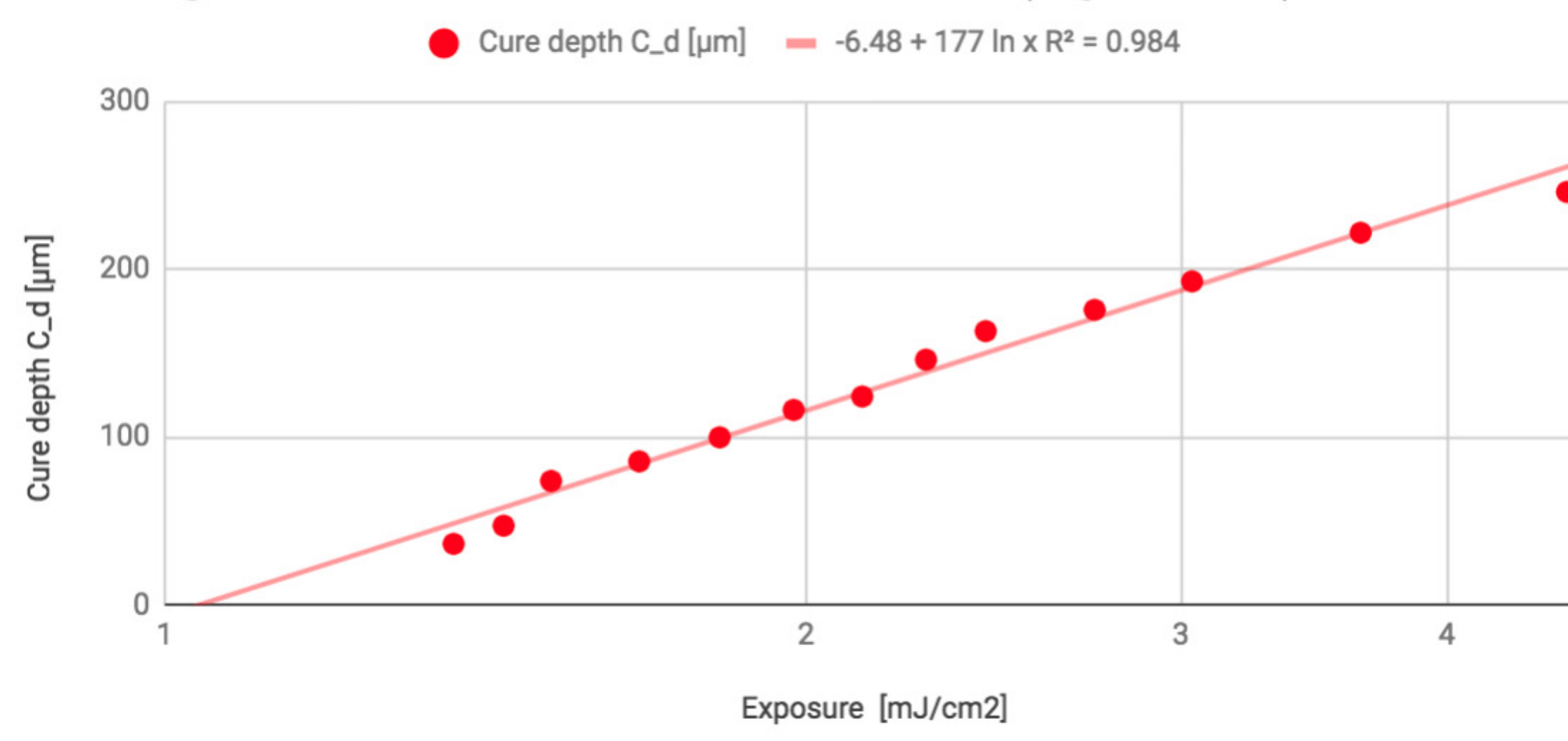


Fig. 3. Working curve for FunToDo Industrial Blend Red. $D_p = 176.61 \mu\text{m}$ & $E_c = 1.037 \text{ mJ/cm}^2$.

Working curve Formlabs High Temp (logarithmic)

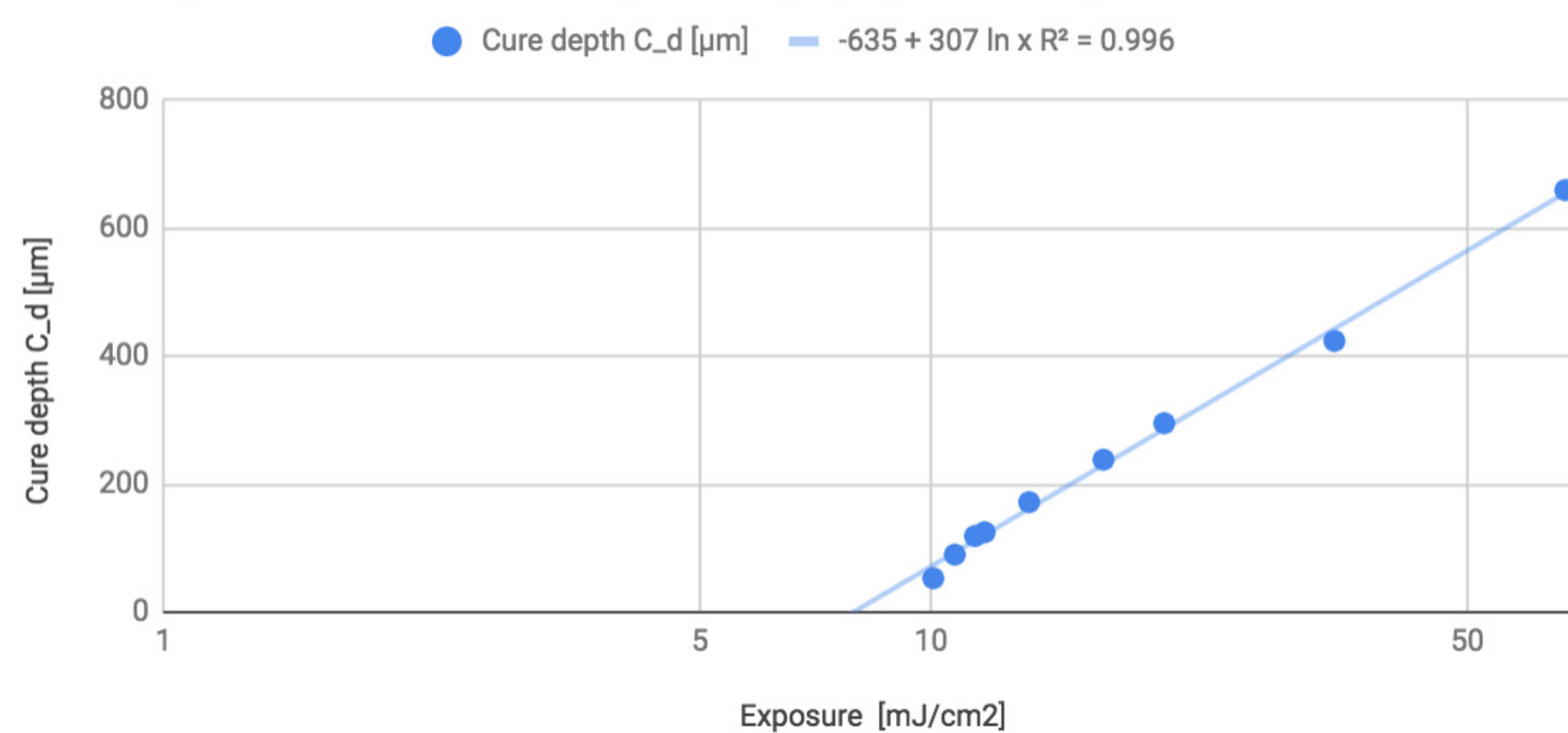


Fig. 4. Working curve for Formlabs High Temperature Resin. $D_p = 306.71 \mu\text{m}$ & $E_c = 7.92 \text{ mJ/cm}^2$.

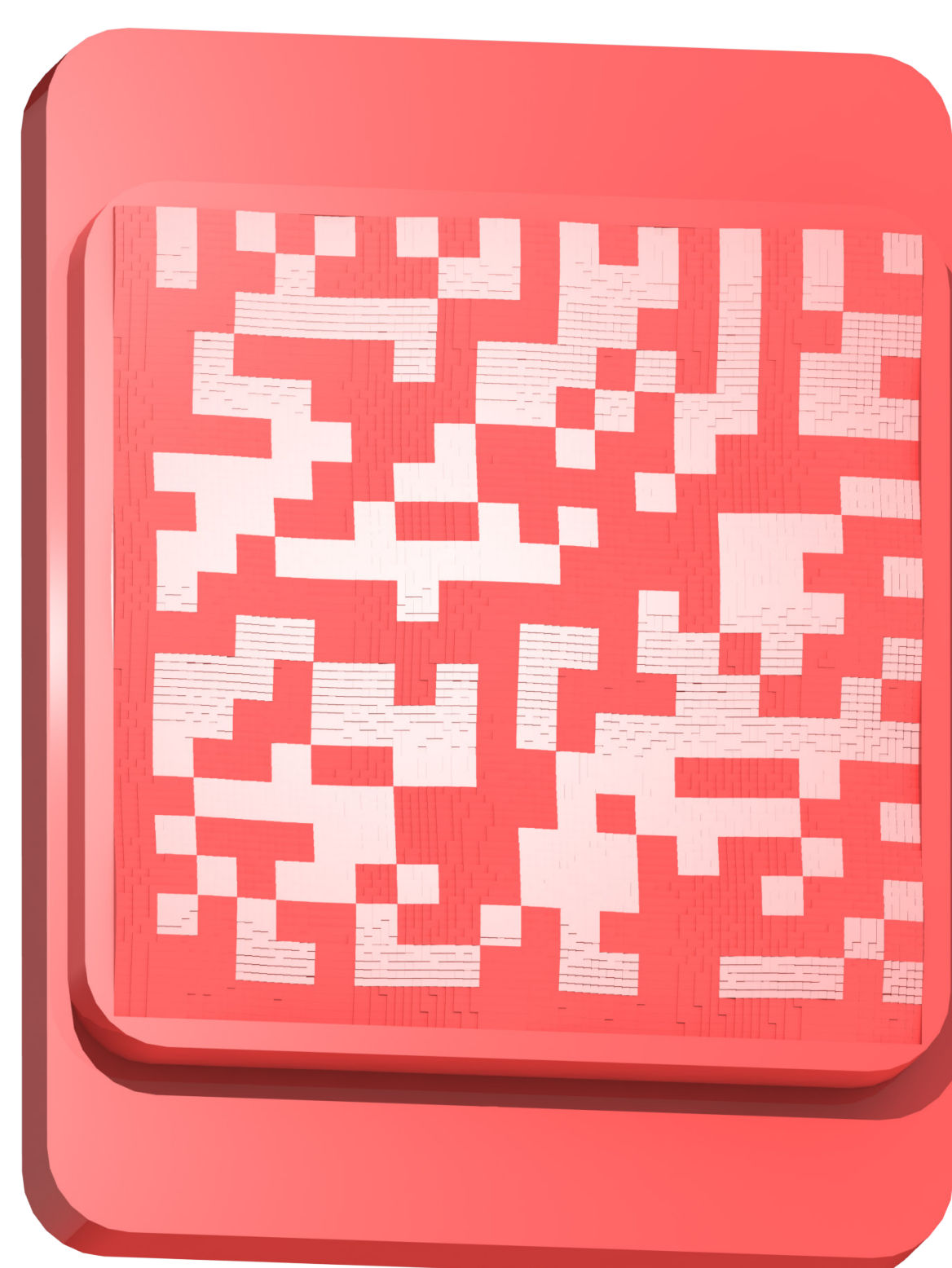


Fig. 5. CAD render of final insert with reflectance elements and mounting flanges on top and bottom. Viewed 10° to light source angle.

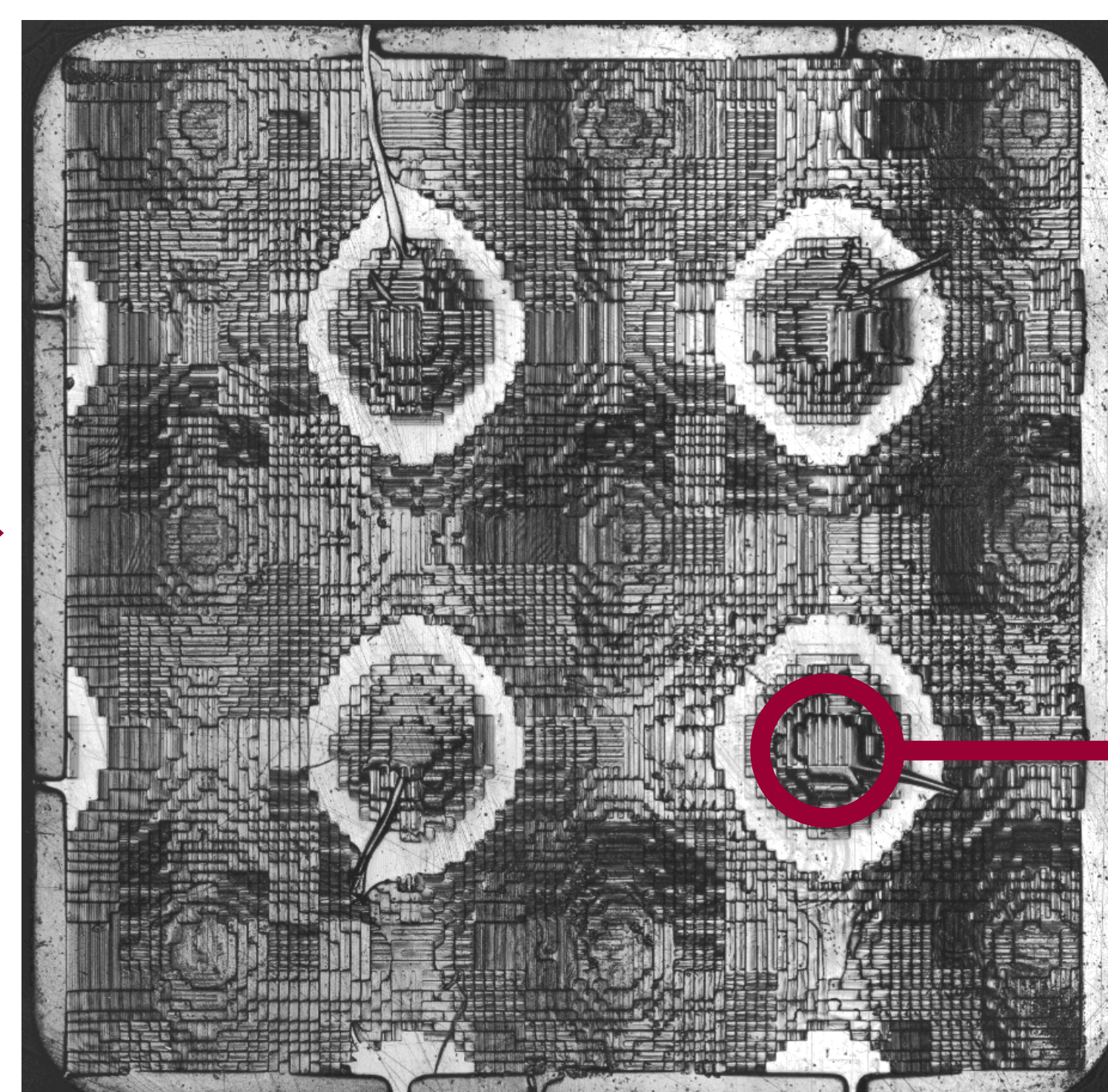


Fig. 6. Confocal microscope image of printed insert with reflectance elements. Notice the ring-formed defects as well as the gashes outward from the four central valleys.

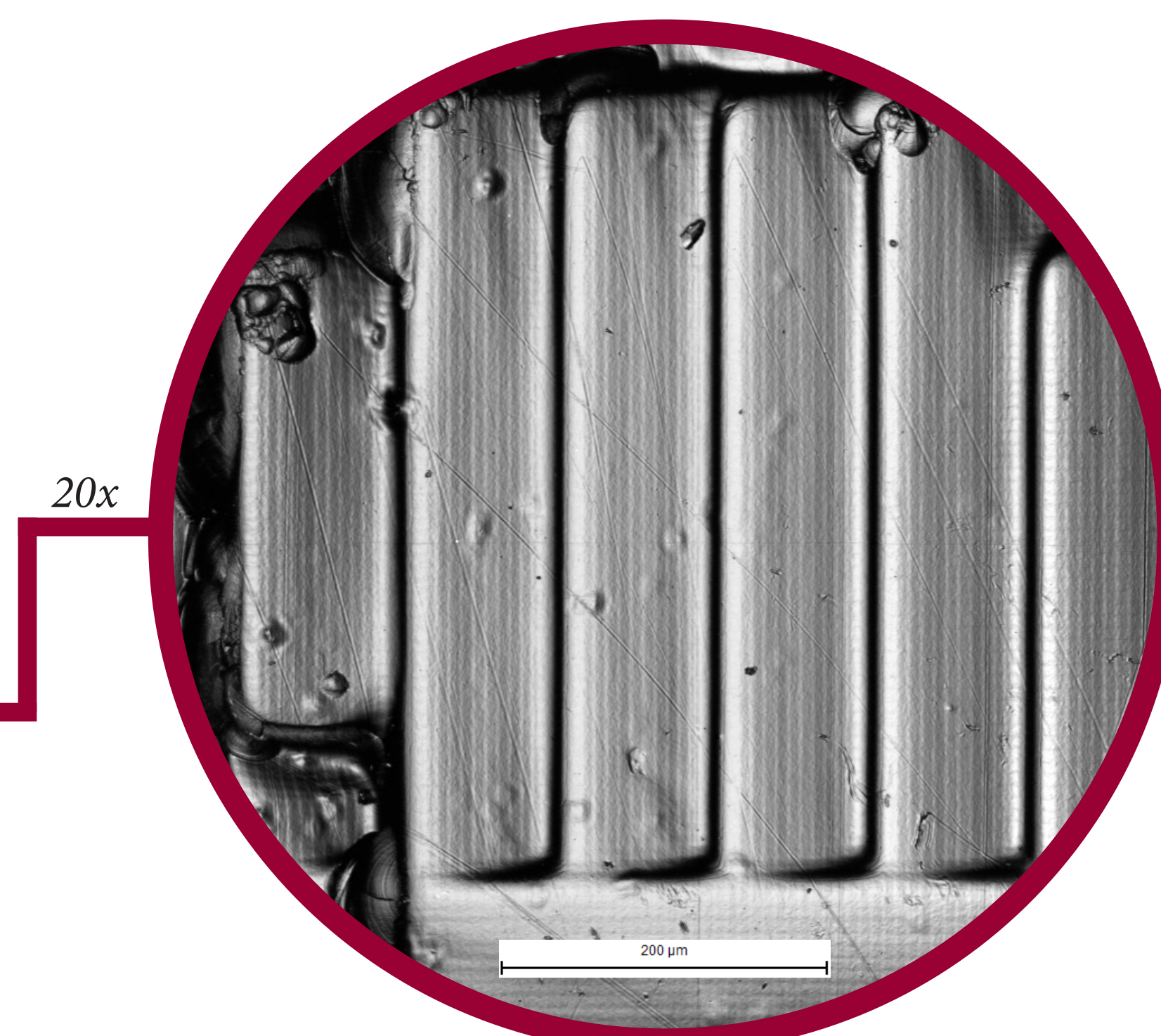


Fig. 7. Top: CLSM zoom-in on the triangular prism reflectance elements. Bottom: Profilometry image generated by SPIP 6.7.5.

Surface Roughness - ISO 4287			
Vertical		Horizontal	
Mean R_a [nm]	44	Mean R_a [nm]	32
Std. R_a [nm]	35	Std. R_a [nm]	04
Mean R_z [nm]	222	Mean R_z [nm]	157
Std. R_z [nm]	163	Std. R_z [nm]	37

Tab. 1: Mean roughness values for the surface depicted in Fig. 7 by either horizontal or vertical measurement.

Acknowledgements

This paper reports work undertaken in the context of project 5163-00001B funded by Innovation Fund Denmark